A New Catalog of Explosion Source Parameters in the Utah Region with Application to M_L–M_C-Based Depth Discrimination at Local Distances

Jonathan R. Voyles[1], Monique M. Holt[1], J. Mark Hale[1], Keith D. Koper[*1], Relu Burlacu[1], and Derrick J. A. Chambers[2]

Abstract

A catalog of explosion source parameters is valuable for testing methods of source classification in seismically active regions. We develop a manually reviewed catalog of explosions in the Utah region for 1 October 2012 to 30 June 2018 and use it to assess a newly proposed, magnitude-based depth discriminant. Within the Utah region we define 26 event clusters that are primarily associated with mine blasts but also include explosions from weapons testing and disposal. The catalog refinement process consists of confirming the explosion source labels, revising the local (M_L) and coda duration (M_C) magnitudes, and relocating the hypocenters. The primary features used to determine source labels are waveform characteristics such as frequency content, the proximity of the preliminary epicenter to a permitted blast region, the time of day, and prior notification from mine operators. We reviewed 2199 seismic events of which 1545 are explosions, 459 are local earthquakes, and 195 are other event types. Of the reviewed events, 127 (5.8%) were reclassified with new labels. Over 74% of the reviewed explosions have both M_L and M_C, a sizable improvement over the unreviewed catalog (65%). The mean M_L–M_C value for the new explosion catalog is -0.196 ± 0.017 (95% confidence interval) compared with a previously determined value of 0.048 ± 0.008 for naturally occurring earthquakes in the Utah region. The shallow depths of the explosions lead to enhanced coda production, which in turn leads to anomalously large M_C values. This finding confirms that M_L–M_C is a useful metric for discriminating explosions from deeper tectonic earthquakes in Utah. However, there is significant variation in M_L–M_C among the 26 explosion source regions, suggesting that M_L–M_C observations should be combined with other classification metrics to achieve the best performance in distinguishing explosions from earthquakes.

Cite this article as Voyles, J. R., M. M. Holt, J. M. Hale, K. D. Koper, R. Burlacu, and D. J. A. Chambers (2019). A New Catalog of Explosion Source Parameters in the Utah Region with Application to M_L–M_C-Based Depth Discrimination at Local Distances, *Seismol. Res. Lett.* **91**, 222–236, doi: 10.1785/0220190185.

Introduction

An important task in regional seismic monitoring is distinguishing explosions from earthquakes. Misidentified explosions are problematic because they contaminate earthquake catalogs that are used to assess seismic hazard. Identifying small explosions at local-to-regional distances is also important for monitoring the zero-tolerance Comprehensive Nuclear-Test-Ban Treaty (Bowers and Selby, 2009). In this context, it is especially important to identify common industrial explosions, such as mine blasts, which might otherwise lead to false alarms (Richards *et al.*, 1992; National Research Council, 1998; Stump *et al.*, 2002).

Several methods have been evaluated for seismic identification of mine blasts at local-to-regional distances including *P*/*Lg* amplitude ratios (Kim *et al.*, 1994), *Sg*/*Rg* amplitude ratios (Tibi *et al.*, 2018), *Rg* excitation (Goforth and Bonner, 1995), spectral modulations (Baumgardt and Ziegler, 1988; Arrowsmith *et al.*, 2006), magnitude differences (Zeiler and Velasco, 2009), and spectral deviation from an earthquake source model (Allman *et al.*, 2008). More recently, approaches based on machine learning have shown promise (Linville *et al.*, 2019). Simpler considerations such as a daytime occurrence (Wiemer and Baer, 2000), waveform similarity with previous known explosions

1. Department of Geology and Geophysics, University of Utah, Salt Lake City, Utah, U.S.A.; 2. Spokane Mining Research Division, National Institute for Occupational Safety and Health, Spokane, Washington, U.S.A.

*Corresponding author: koper@seis.utah.edu

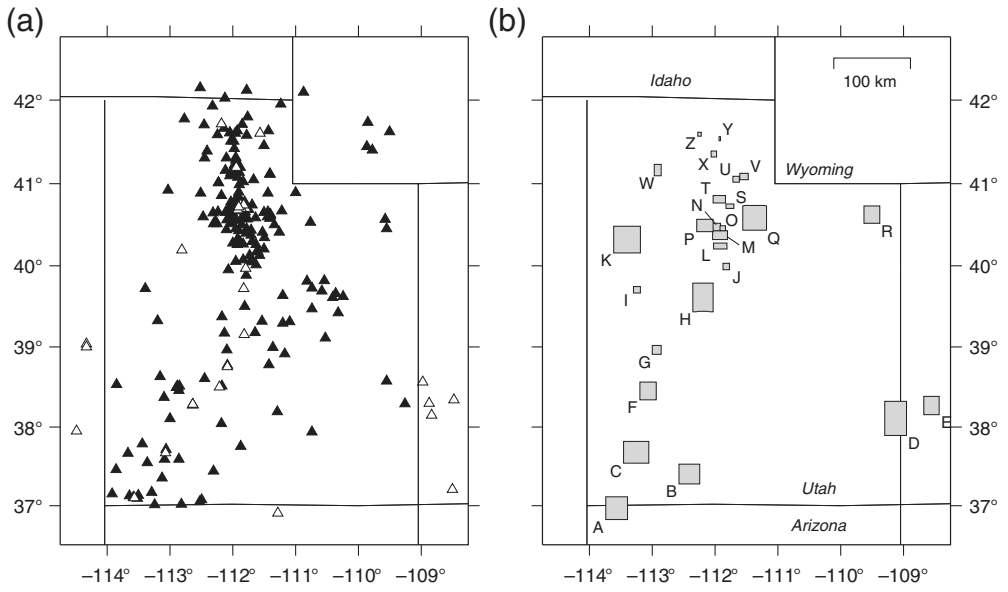

Figure 1. (a) Seismometers used by the University of Utah Seismograph Stations (UUSS) between 2012 and 2018. The UUSS maintains and operates the University of Utah Regional Network (UU; solid triangles) and records data from seismographs in allied networks (open triangles) for seismic processing. (b) The 26 explosion source regions, organized from south to north. The 1545 explosions in these regions occurred between 1 October 2012 and 30 June 2018.

(Gibbons and Ringdal, 2006), and location near a permitted blasting region (Astiz *et al.*, 2014) are also useful for identifying mine blasts.

In this study, we develop a new catalog of explosion source parameters in the Utah region that can be combined with the existing regional earthquake catalog to evaluate methods of source discrimination. We manually review 2199 seismic events that occurred within or adjacent to the Utah region between 1 October 2012 and 30 June 2018. We repick the arrival times, relocate the hypocenters, and recalculate the magnitudes, resulting in revised solutions for 1545 explosions, which are assigned to one of 26 distinct source regions. The explosions are mostly mining-related quarry blasts but include some single-fired, above-ground explosions carried out by government agencies. We use the new catalog to examine the ability of a recently proposed (Koper *et al.*, 2016; Holt *et al.*, 2019) depth discriminant—the difference between local magnitude (M_L) and coda duration magnitude (M_C)—to separate explosions from earthquakes in the Utah region. Previous work found a mean M_L–M_C value of 0.048 ± 0.008 for 3957 tectonic earthquakes in Utah and a mean M_L–M_C value of −0.137 ± 0.008 for 3723 likely explosions in Utah (Koper *et al.*, 2016). Their interpretation was that near-surface explosions are efficient at generating extended coda waves, perhaps because of *Rg* excitation and scattering, leading to anomalously high M_C values.

The waveforms of the likely explosions studied in Koper *et al.* (2016) were analyzed less rigorously than those from events initially classified as earthquakes because the primary mission of the University of Utah Seismograph Stations (UUSS) is mitigating earthquake risk in the Utah region. The epicenters are generally of high quality because they are a factor in the initial source classification process. However, for a given mine region, the arrival times were picked by different analysts over a period of many years. The relative locations can be improved using a single analyst to repick arrival times from events in a given source region at the same time—as we do here. The magnitudes of the likely explosions studied by Koper *et al.* (2016) are generally of lesser quality than those of earthquakes characterized by UUSS because magnitudes are not used in the initial source classification process. The careful waveform reanalysis we do here leads to more accurate magnitudes and helps us identify any misclassified events, in turn leading to a more rigorous evaluation of M_L–M_C as a source classifier.

Seismic Monitoring in the Utah Region

The University of Utah Seismograph Stations (UUSS) operates the University of Utah Regional Seismic Network (UU; University of Utah, 1962), which, as of 30 June 2018, consisted of 39 broadband, 67 short-period, and 78 strong-motion seismometers (Fig. 1). Continuous seismic data from this network are telemetered to the UUSS earthquake information center and combined with data recorded from neighboring seismic networks to detect, locate, and characterize seismic events. This process uses the ANSS Quake Management System (AQMS) software package, in which ANSS is the Advanced National Seismic System. All automatically generated AQMS solutions are reviewed and refined by UUSS analysts. For AQMS solutions with magnitudes larger than **M** 2.5–3.5, depending on the region, a duty seismologist reviews the event within 30–60 minutes and submits refined earthquake solutions to the ANSS Comprehensive Earthquake Catalog. UUSS also publishes online reports with finalized earthquake solutions on a quarterly basis (see Data and Resources).

The UUSS uses M_L and M_C to describe the magnitude of small earthquakes. M_L is calculated from the horizontal channels of broadband stations using the equation:

$$M_L = \log_{10}[A] - \log_{10}[A_0] + S, \quad (1)$$

in which A is half of the sum of the maximum north–south channel peak-to-peak amplitude (mm) for a single cycle divided by two and the maximum east–west channel peak-to-peak amplitude (mm) for a single cycle divided by two on an emulated Wood–Anderson seismograph, $\log_{10}[A_0]$ is an empirical distance correction, and S is an empirical station correction (Pechmann *et al.*, 2007). M_C is calculated from the vertical channel of short-period or filtered broadband stations using the equation:

$$M_C = -2.25 + 2.32\log_{10}[\tau] + 0.0023\Delta, \quad (2)$$

in which τ is measured as the time difference in seconds from the *P*-wave arrival to the time that the average absolute value of the ground velocity drops below 0.01724 μm/s, and Δ is the epicentral distance in kilometers (J. C. Pechmann, personal comm., 2019).

An important task for UUSS analysts is determining whether an automatically detected seismic event in the AQMS database is an earthquake (local, regional, or teleseismic), a likely explosion, or a noise trigger. Because the UUSS mission focuses on reducing earthquake risk in Utah, AQMS solutions determined to be explosions are reviewed with less stringent quality criteria and excluded from the UUSS earthquake catalog. An analyst classifies a reviewed AQMS solution as a likely explosion if its epicenter is within or very near a permitted blasting region, if it occurred during daylight hours (typically 13:00–03:00 UTC) when surface blasting is permitted in Utah, if its waveforms look similar to those of previous explosions in the area, or if UUSS is given prior notification from the mine operator. In the AQMS database, these events are labeled either as "qb" for quarry blast or "EX" for explosion. For convenience, in this article we refer to all such events as "LE" for likely explosion.

There are two types of explosions that are most prominent in Utah: (1) disposal and testing of military weapons and (2) quarry blasts. The most common military explosions involve the above-ground destruction of rocket motors at the Utah Test and Training Range (Stump *et al.*, 2007). A smaller number of military-related above-ground explosions are carried out at Dugway Proving Ground (DPG, see Data and Resources). Non-military surface blasts, shallow ripple-fired blasts, and shallow single-fired blasts are generally used to develop resources such as precious metals, minerals, and gravel and are classified as quarry blasts. In 2010, a list of Utah mines with active permits for surface blasting was obtained from the Utah Division of Oil, Gas, and Mining (see Data and Resources). The list was incorporated into the AQMS to aid UUSS analysts. If an analyst-refined event epicenter is located within either 5 or 20 km of a permitted mine, depending on the station coverage in that area, AQMS alerts the analyst that the event might be an explosion. The AQMS-generated nearby-mine warning can bias the analyst toward an explosion label because a nearby mine warning frequently coincides with an actual explosion.

As a result, LEs are usually confined to the areas around known, active mines. An LE that does not locate near one of these mines could have an inaccurate location from analyst error or could be associated with a mine that has infrequent or small explosions.

Reanalysis of Likely Explosions

Since 1 October 2012, when UUSS started using AQMS software, thousands of likely explosions have been recorded. In this study, we reanalyze these events with the goal of confirming their source type and refining their magnitudes and, when appropriate, their locations. Generally, first arrival picks on LE waveforms are made with the same standards as those for earthquake waveforms. This is because part of the initial classification process uses the proximity of the epicenter to active mines as a criterion. However, the majority of explosion magnitudes are automated AQMS solutions, which are less robust. Therefore, our reanalysis was more heavily focused on improving magnitude estimations.

Because analysts work on events chronologically, as they occur, it is reasonable to reanalyze the LEs in this manner. However, reanalyzing LEs chronologically recreates the same problem the original analysts faced—the wide geographic distribution of the various sources makes event classification challenging. To mitigate this issue and increase the accuracy of our findings, we reanalyze LEs geographically. The first step is an examination of all seismicity within a defined latitude and longitude range encompassing a known blasting region to establish a qualitative understanding of the waveform differences between earthquakes (EQ) and explosions (EX) in that area. This is the most valuable tool in differentiating and labeling source types correctly because earthquakes and explosions that occur in the same geologic setting generally have distinct waveforms (Fig. 2). Other factors considered for source classification include preliminary epicentral location, *P*-wave first motions, and time of day. Unlike near-surface blasting, underground blasting is not limited to daylight hours, but these blasts are typically much smaller than surface blasts and unlikely to trigger the regional network. Other classification tools include checking for acoustic arrivals on seismic stations and communicating with mine operators for ground truth information.

Reclassification results in one of five outcomes. An event that was originally classified as an earthquake and remains classified as an earthquake upon reanalysis is described as a true positive (TQ); if the event is reclassified as an explosion, then it is described as a false positive (FQ). An event that was originally classified as an explosion and kept as an explosion is described as a true negative (TX), whereas the same event reclassified as an earthquake is described as a false negative (FX). If the reclassification of an event cannot be described with this scheme, then the

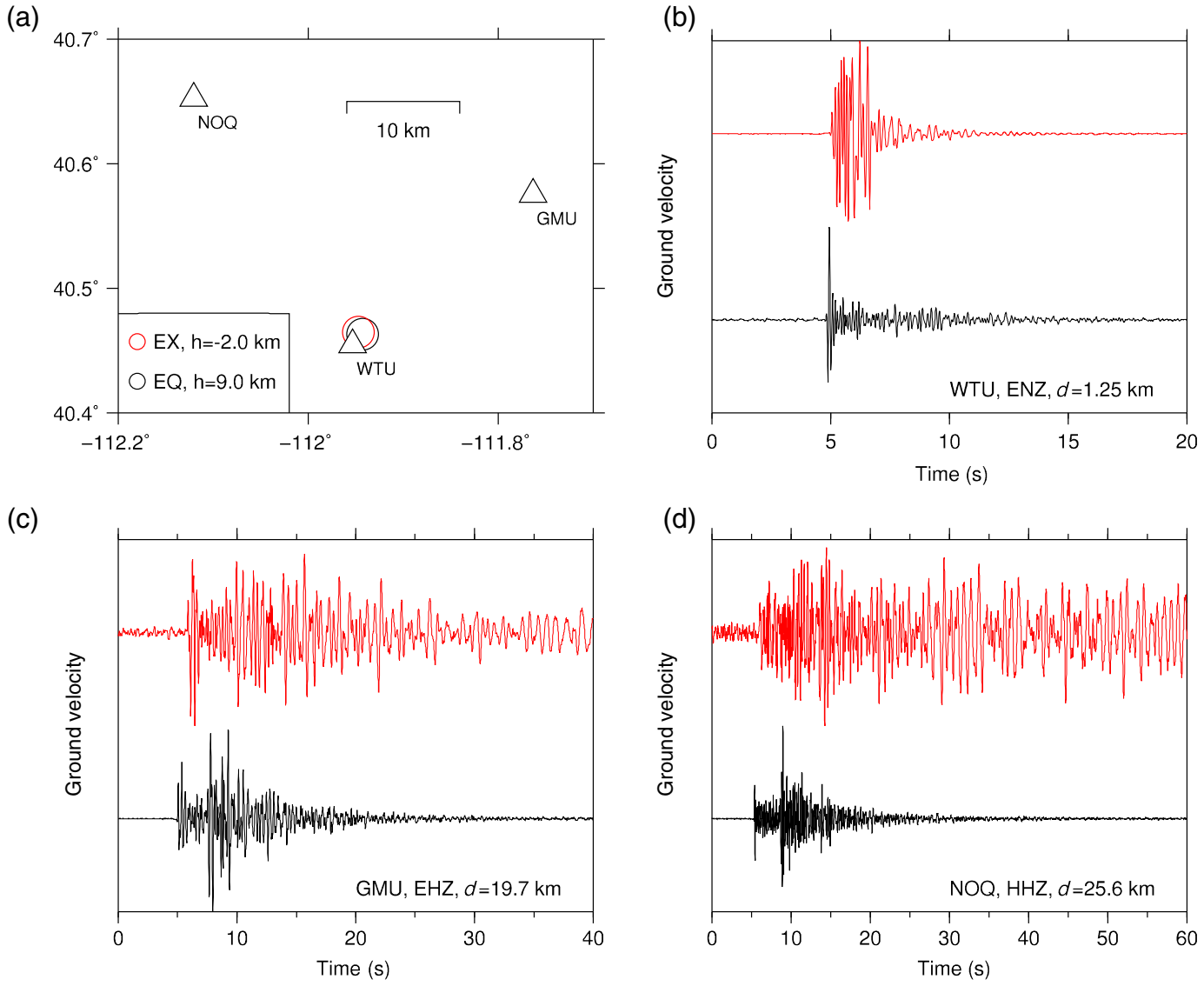

Figure 2. (a) Locations of a quarry blast (red) and naturally occurring earthquake (black) that have nearly identical epicenters. The quarry blast occurred on 14 October 2014 at 20:13:22 (UTC) with magnitudes of 1.41 M_L and 1.81 M_C and a depth of −2.0 km. The earthquake occurred on 25 June 2017 at 21:20:10 (UTC) with magnitudes of 1.95 M_L and 2.02 M_C and a depth of 9.0 km. Vertical component waveforms are shown for stations (b) UU.WTU, (c) UU.GMU, and (d) UU.NOQ. All waveforms are proportional to ground velocity and have been bandpassed at 1–10 Hz. Each trace is individually normalized in the given time window. The average epicentral distance, *d*, from the co-located events is reported in the bottom of each panel. EH, short-period sensors; EN, strong motion accelerometers; EQ, earthquakes; EX, explosions; HH, broad-band sensors; Z, vertical component. The color version of this figure is available only in the electronic edition.

event is labeled as "other" (O). Teleseismic events, noise triggers, and poorly recorded events are examples of "other" classifications.

Once the event type is determined, we reevaluate peak-to-peak amplitude measurements for M_L determination, signal duration measurements for M_C determination, and arrival time picks for hypocenter determination. After all picks and measurements have been reviewed, we relocate the event, recalculate the associated magnitudes, and save the event to the AQMS database. Locations are calculated using HYPOINVERSE (Klein, 2002) with a set of region-specific 1D velocity models. Depth control is limited for blasts because of the rarity of discernable *S* waves and the low density of seismometers near blasting sites. Therefore, most explosions in our database are located with fixed depths of 2 km above sea level ($h = -2$ km), which is the approximate average elevation of permitted mines listed by the Utah Division of Oil, Gas, and Mining.

Results

In Table 1, we summarize the outcome of the reanalysis for each of the 26 geographical clusters shown in Figure 1. We report the total number of reviewed events and subtotals in each of the five classes: TQ, FQ, TX, FX, and O. We assess the quality of the original source labels using binary classification theory. Sensitivity measures the rate of true positives and is given by TQ/(TQ+FX), which varies between 0 and 1. High sensitivity

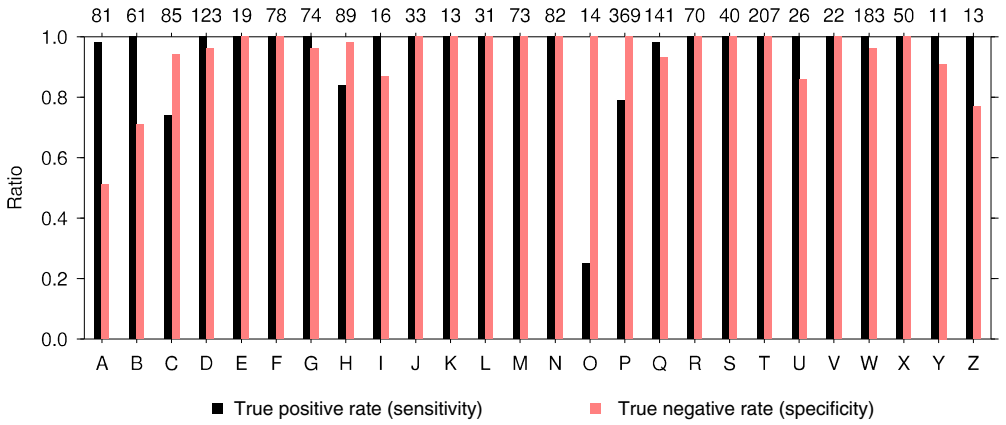

Figure 3. Variation in sensitivity and specificity of the original UUSS analyst classification of source type. For sensitivity, a ratio of 1.0 means that no earthquakes were originally misclassified as explosions. For specificity, a ratio of 1.0 means that no explosions were originally misclassified as earthquakes. The total number of earthquakes and explosions reviewed in each region are listed across the top x axis. The color version of this figure is available only in the electronic edition.

means that UUSS analysts missed very few actual earthquakes in their original analysis. Specificity measures the rate of true negatives and in our nomenclature is given by TX/(TX+FQ), which also varies between 0 and 1. High specificity means that very few explosions were originally misclassified as earthquakes by UUSS analysts. For the 2004 reviewed events that were not labeled O, the original analyst classifications had a sensitivity of 0.92 and a specificity of 0.96. Figure 3 illustrates the variation in sensitivity and specificity from region to region. Note that for regions with no TQs, the sensitivity is reported as 1.00.

In Table 1, we also report the number of explosions with valid magnitude estimates for both M_L and M_C in each region. Overall, we were able to estimate both magnitudes for 1148 of the 1545 explosions. For explosions occurring in sparsely instrumented portions of the Utah region, it was often difficult to estimate M_L because of the lack of nearby broadband stations with calibrated M_L station corrections. Very small explosions were also problematic because of the relative sparsity of broadband stations. In the following, we give details about each geographical cluster as defined in Figure 1.

Region A

Region A is located in the southwest corner of Utah on the border with Arizona. Station coverage is heavily biased toward the north-northeast leading to an average azimuthal gap (AAG) of 196° in the relocations. The nearest broadband station is UU.LCMT (where UU is the network code and LCMT is the station code), which is located about 10 km east of the event cluster. Large amplitude, low-frequency surface-wave content (*Rg*) is characteristic of the explosion waveforms. We reviewed 81 seismic events in this cluster and identified 41 as explosions, 21 of which were originally identified as explosions (TX) and 20 of which were originally misclassified as earthquakes (FQ). This was the highest fraction of false positives for any region. While the sensitivity of the original analyst classifications was higher than average at 0.98, the specificity was the lowest in any of the 26 regions at 0.51.

Region B

Region B is located in southern Utah about 150 km northeast of region A. Station coverage is again biased, to the north and west, but the coverage is more uniform than in region A and the AAG is correspondingly lower at 125°. The nearest broadband station is UU.PKCU, which is located only 5–10 km to the east of the event cluster. Emergent, spindle-shaped waveforms are again observed for the explosion waveforms. The original classifications had a perfect sensitivity of 1.00, but again a relatively low specificity of 0.71.

Region C

Region C is located is southwestern Utah with station coverage concentrated to the south and east, yielding an AAG of 147°. The nearest broadband station is UU.SZCU, which is located about 20 km east of the event cluster. The original analyst classifications had lower than average sensitivity (0.74). After thorough reanalysis, including conversations with mine operators, 18 events that were originally classified as explosions were changed to earthquakes. In general, the misclassified earthquakes had emergent *P* waves, which made it difficult to determine first motions; however, these waveforms also tended to have impulsive *S* waves that were absent on the explosion waveforms. This was the only region in which M_L and M_C estimates could be made for all the verified explosions.

Region D

Region D is southwest of the Paradox Valley area in western Colorado, a region that experiences induced earthquakes from fluid injection (Fig. 4; Block *et al.*, 2015; Yeck *et al.*, 2015; King *et al.*, 2016). The Bureau of Reclamation runs a small aperture network (RE) in the region to monitor the induced seismicity. The network began recording in 1985 and has recently been updated with 20 broadband three-component seismometers. Station RE.PV05 is within 1–2 km of the cluster of explosion sources, which are located about 20 km south-southwest of the injection well—where the induced earthquakes are concentrated. The nearest UUSS station is UU.CRLU, which is located about 10 km to the north-northwest of the explosion cluster.

TABLE 1
Reclassification Results by Source Region

Source Region	Number of Reviewed Events	EQs Kept as EQs (TQ)	EQs Changed to EXs (FQ)	EXs Kept as EXs (TX)	EXs Changed to EQs (FX)	Sensitivity TQ/(TQ+FX)	Specificity TX/(FQ+TX)	Other* (O)	EXs with M_L and M_C
A	81	39	20	21	1	0.98	0.51	0	37
B	61	40	6	15	0	1.00	0.71	0	19
C	92	50	1	16	18	0.74	0.94	7	17
D	130	23	4	96	0	1.00	0.96	7	37
E	19	0	0	19	0	1.00	1.00	0	5
F	79	17	0	61	0	1.00	1.00	1	13
G	74	0	3	71	0	1.00	0.96	0	31
H	90	32	1	50	6	0.84	0.98	1	44
I	18	1	2	13	0	1.00	0.87	2	1
J	33	15	0	18	0	1.00	1.00	0	14
K	13	4	0	9	0	1.00	1.00	0	7
L	31	1	0	30	0	1.00	1.00	0	19
M	80	3	0	70	0	1.00	1.00	7	53
N	85	41	0	41	0	1.00	1.00	3	34
O	14	1	0	10	3	0.25	1.00	0	9
P	409	22	1	340	6	0.79	1.00	40	316
Q	144	95	3	41	2	0.98	0.93	3	4
R	188	3	0	67	0	1.00	1.00	118	66
S	41	0	0	40	0	1.00	1.00	1	26
T	209	7	0	200	0	1.00	1.00	2	180
U	27	4	3	19	0	1.00	0.86	1	9
V	23	8	0	14	0	1.00	1.00	1	7
W	183	0	8	175	0	1.00	0.96	0	172
X	50	17	0	33	0	1.00	1.00	0	23
Y	12	0	1	10	0	1.00	0.91	1	1
Z	13	0	3	10	0	1.00	0.77	0	4
Totals	2199	423	56	1489	36	0.92	0.96	195	1148

*This category includes regional, teleseismic, and unknown events, either correctly or incorrectly initially classified, in addition to duplicate events in the database, or events with data quality too poor to analyze. EQ, earthquakes; EX, explosions.

It consists of three strong-motion channels and a short-period, vertical component channel.

In comparison with regions A–C, region D has a much lower percentage, 18% (Table 1), of total events that are earthquakes (natural and induced). A typical explosion waveform here has large amplitude surface waves and clear changes in frequency content over time—a higher frequency *P*-wave packet is followed by a lower-frequency surface wave (*Rg*) train. At greater distances, these waveforms become very emergent, which contributes to less accurate locations. The emergent nature of the first arrivals resulted in four events initially classified as EQ being reclassified as EX. Overall, the specificity was still quite high at 0.96, and the sensitivity was 1.00—indicating that no earthquakes were missed during the original analysis.

Region E

Similar to region D, region E is located in western Colorado near Paradox Valley, about 30 km east of the injection well.

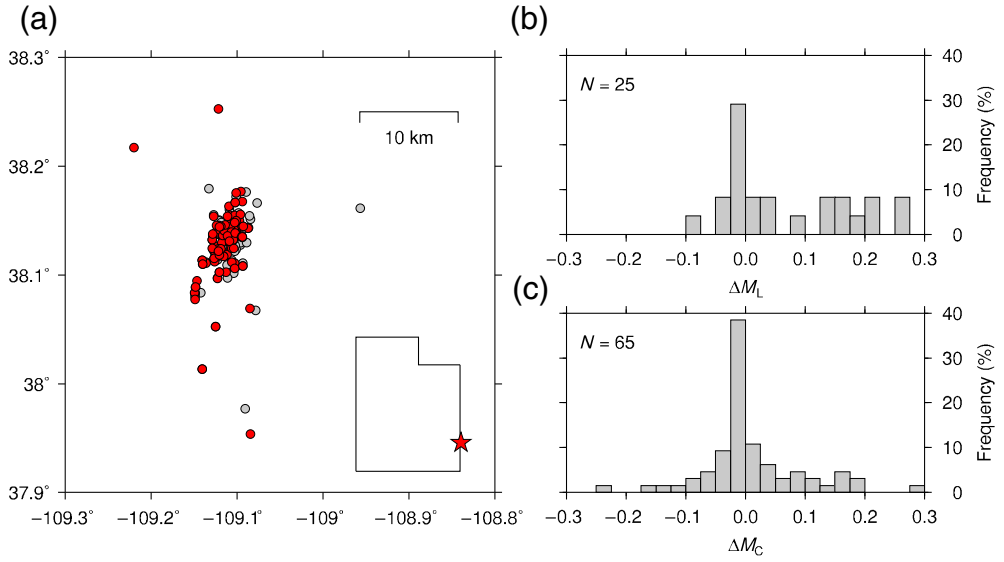

Figure 4. (a) Map of region D with explosions plotted to reflect their epicenters before (gray) and after (red) reanalysis. The location of region D within the Utah region is indicated by the red star on the inset image of the state. Changes in (b) M_L and (c) M_C during reanalysis. The color version of this figure is available only in the electronic edition.

The nearest station, RE.PV15, is a few kilometers to the northeast of the explosions. In contrast to region D, the waveforms from region E have strongly impulsive first arrivals. The waveform quality, distinct geographical location, and different closest stations are what distinguish this cluster from region D. This region exhibits a notable lack of earthquakes (natural and induced). There were no sources in this region that were originally misclassified.

Region F

Region F is located in southwestern Utah near a region of high heat flow that is the site of a Department of Energy funded project called Frontier Observatory for Research in Geothermal Energy (FORGE, Pankow *et al.*, 2017). UUSS station coverage is very good in this area with four new broadband stations installed within 20 km of the explosion cluster during the last several years. Several other short-period stations have long been sited within about 40 km of the cluster. Of 17 earthquakes and 61 explosions that were reanalyzed, none were misclassified. The explosion waveforms in this region were quite distinct from earthquake waveforms.

Region G

Region G in west-central Utah is an area with infrequent natural seismicity. The closest broadband station, UU.SWUT, is located about 50 km to the north-northwest of the explosion cluster. These explosion waveforms exhibit particularly impulsive *P* waves, high-amplitude *S* waves, and less distinctive *Rg* waves than the explosion waveforms in most other regions. The waveforms at the closest station, IMU, are very consistent leading to few misclassified events. However, the atypical *Rg* waves resulted in three FQ reclassifications, as surface-wave propagation here is more similar to that of an earthquake than an explosion. Nevertheless, specificity was high at 0.96.

Region H

Region H is located in central Utah and exhibits three distinct subclusters of explosions. The nearest broadband station, UU.NLU, is located 20–40 km north of the seismicity. Station coverage is good, with the only gap to the southwest. The southernmost subcluster exhibits typical explosion waveforms with consistent frequency content. Events in the two northern clusters have waveforms with surface waves of longer duration and lower frequency. This discrepancy contributed to six FX reclassifications (missed earthquakes) and a sensitivity of only 0.84. The specificity was excellent at 0.98.

Region I

Region I is located in a sparsely instrumented part of west-central Utah. The nearest broadband station, US.DUG, is located about 75 km to the northeast. A short-period vertical-component station, UU.FSU, is located about 5 km to the west. The explosion waveforms are very distinct from earthquake waveforms in this region. We used the *P* and *S* arrival-time moveout from the closest station, UU.FSU, to a farther station, UU.FLU, to distinguish earthquakes from explosions in region I. The separation of the body waves at distance allows the analyst to observe the energy of *S* relative to *P* and make a more confident choice of event type. Sensitivity and specificity were both high.

Region J

Region J is located in a densely instrumented part of central Utah. The nearest broadband station, UU.MPU, is located 5–10 km to the east, and a second broadband station, UU.NLU, is located 10–15 km to the west. Perhaps because of the good station coverage, none of the 33 events were reclassified.

Region K

Region K is one of two areas in our catalog that is subject to periodic weapons testing and disposal. It is located in west-central

Utah and contains the U.S. Army DPG. UUSS has a working relationship with DPG and has ground truth information (test confirmation and payload description) for eight of the nine explosions recorded in this region. UUSS is familiar with DPG explosive practices, and the event depths in this region are fixed to −1.3 km, the elevation of the test site. Dugway explosions typically have an emergent first arrival and a highly energetic, long-duration surface wavetrain. These explosions are best recorded on station UU.DUG, deployed on DPG but about 20–30 km east of the seismic events. Though UUSS has ground truth for DPG events, high-accuracy seismic locations can be difficult to determine because of station gaps to the north and west. No events were misclassified in this region.

Region L

Region L is in an area of central-northern Utah with dense station coverage but infrequent natural seismicity. The nearest broadband station, UU.MPU, is located about 15 km southeast of the cluster, and five other stations are located at shorter distances. Natural earthquakes are infrequent in this area, and only 1 of the 31 events reviewed here was an earthquake. None of the events were misclassified.

Region M

Similar to region L, region M is located in an area of central Utah with infrequent natural seismicity (3 EQ vs. 70 EX). The relocated epicenters cluster tightly but with some northwest–southeast scatter. Two broadband stations, UU.NLU and UU.MPU, are located within 40 km of the event cluster. There are seven type-O events here, which are poorly recorded, small-magnitude LEs. The EX waveforms are consistent from event to event and with other mines (emergent arrivals, frequency content, and decay rate). The low rate of natural seismicity and the consistency of the waveforms contributed to there being no misclassifications.

Region N

Region N is located in north-central Utah in a densely instrumented part of the network. The nearest broadband, UU.NOQ, is about 15 km northwest of the seismicity, but nearly 10 other seismograph stations are located at similar or closer distances. This region encompasses a mine as well as an earthquake swarm that occurred in June 2017, leading to a perfect balance of source types (41 EQ and 41 EX). There were no misclassifications in this region.

Region O

Region O is near regions M and N and is an area of dense station coverage. This coverage outweighs the low magnitude of the explosions, which allows for 90% of the events to have calculable M_L and M_C values. The first arrivals at station UU.WTU are emergent, leading to relatively dispersed epicenters for this region. UU.WTU is used in tandem with UU.GMU for discrimination based on phase moveout. Even with a low rate of seismicity, there are three FX reclassifications, giving a sensitivity of 0.25, the lowest in any region. The *P*-wave frequency content and *S*-wave frequency content for some of the blasts in this region looked similar to that of an earthquake, but these events were correctly classified after finding subtle similarities in waveform characteristics between the events when all were simultaneously compared.

Region P

Region P is located in the Oquirrh mountain range in north-central Utah (Fig. 5). The nearest broadband station, UU.NOQ, is 5–10 km to the north of the clustered seismicity. Region P contains one of the largest open pit mines in the world, which is a source of frequent explosions. A variety of blasting practices are used to mine primarily porphyry copper and other precious metals such as gold and molybdenum. Dense station coverage and the relatively large magnitude of these events result in well-constrained locations. There is only one FQ (specificity ∼1.0) because UUSS analysts are very familiar with this mine. In contrast, there are a significant number of FXs (6), leading to a relatively low sensitivity of 0.79. This is likely due to the 70:1 ratio of LEs to earthquakes in this region.

The 2817 LEs in region P required a different analysis strategy than the other regions. We chose to evaluate every tenth explosion in chronological order for efficiency. Through selecting a subset chronologically, we believed we would get a representative sample of epicenters, magnitudes, blasting practices, and times of day for the LEs. In this region, three stations are used to verify that an event is from this mine. UU.MID is normally the closest station to an event, and UU.CWU and UU.NOQ, while farther away, also have clear waveforms.

Although only a tenth of all region P LEs were carefully analyzed, every remaining event was briefly checked for duplication and time of day. Duplication of events occurs in other mining regions but was most commonly observed in region P. Occasionally, an event is large enough to trigger the AQMS automatic procedure, and this automatic solution is not reviewed by an analyst. The analyst may then process a separate trigger with the same event and two solutions will exist in the database. This occurred for 25 events in region P.

Region Q

Region Q is in north-central Utah about 50 km east of region P but still within the densest portion of the UUSS regional network. The broadband station UU.JLU is within the LE cluster, which is relatively dispersed compared with the tight epicentral clustering observed in other regions. Region Q events are processed as having three indistinct subclusters of seismic activity: two east–west lineations (subclusters I and II) and a southern group of events (subcluster III). Subcluster I is the northernmost subset of events within this region, and its seismicity is best recorded on UU.RCJ. The explosion waveforms typically

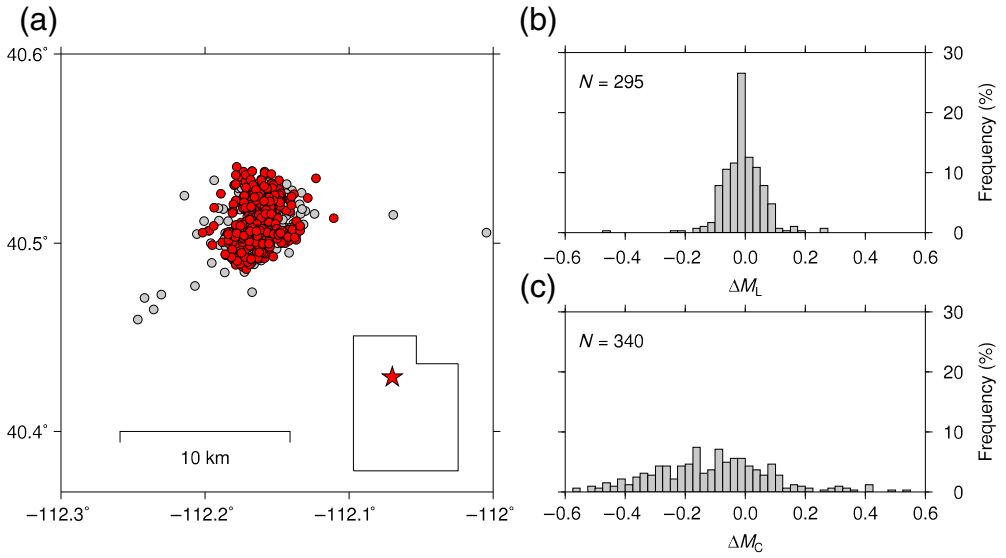

Figure 5. (a) Map of region P with explosions plotted to reflect their epicenters before (gray) and after (red) reanalysis. The location of region P within the Utah region is indicated by the red star on the inset image of the state. Changes in (b) M_L and (c) M_C during reanalysis. The color version of this figure is available only in the electronic edition.

have high-amplitude, low-frequency, impulsively arriving, and quickly decaying surface waves. Events within subcluster II can be described as more emergent and smaller amplitude than subcluster I. These events are often well recorded on UU.KLJ and UU.JLU. Subcluster III events demonstrate clear frequency changes upon the arrival of *S* waves. Station UU.HEB records the highest quality waveforms for these LEs. Both sensitivity (0.98) and specificity (0.93) are high in this region.

Region R

Region R is in the northeastern corner of Utah where station density is low, leading to an AAG of 200 (Fig. 6). Broadband station UU.RDMU, however, is located adjacent to the southern edge of the LE cluster. Region R contains an active phosphate mine. Natural earthquakes are infrequent in this region, and all the events were correctly classified. Additionally, 99% of events had both an M_L and M_C measurement, making region R among the top two mines with both M_L and M_C values. This is mainly owing to the large size of the events here.

This mine sets off explosives in double shots, an uncommon practice in Utah. The majority of shots have an eight second delay, plus or minus a few seconds. Only station UU.RDMU was close enough to consistently record the double shots clearly, though they are occasionally visible at UU.VNL. We limit our reanalysis to 67 of the 185 LEs in region R: single blasts (very infrequent), double blasts with enough delay (~10 s) to distinguish the two shots, and double blasts that essentially overlap but have a larger second shot. The goal is to avoid double shots that are indistinguishable since they would yield an artificially high M_C. Events with an unclear number of shots, unrecorded on UU.RDMU, or both are not analyzed. Double shots from this mine can look similar to earthquakes; the *P* wave of the second shot can look like the *S* wave of the first shot. The analyst looks for the number of phases as distance increases. An earthquake recorded at local distances will have two distinct body wave phases (*P* and *S*), whereas a double blast would yield four phases (*P* and *S* for each blast).

Region S

Region S is located in north-central Utah where station density is highest. The nearest broadband station, UU.CTU, is within a few kilometers of the LE cluster. Good station coverage (65% of events have M_L and M_C estimates) and extremely clear, consistent, and blast-like waveforms at UU.CTU contribute toward making confident classifications (specificity of 1.00). There were no natural earthquakes in region S during the time period covered in this study.

Region T

Region T is nearby region S and includes one of the quarries that UUSS analysts are very familiar with (Fig. 7). This familiarity results in no event reclassifications in this region. UU.HRU, the closest station to most of the event epicenters, and UU.RBU are used in tandem for classification. Along with region N, region T also encompasses an earthquake swarm, which included seven events located southwest of the LE cluster in March 2012. Over 90% of the 200 events have both M_L and M_C. In general, the strong overall station coverage outweighs the small size of the events and results in well-constrained epicenters and magnitudes.

Region U

Region U is also in the high-density portion of the UUSS regional network about 20 km northeast of region T. The nearest broadband station, UU.CTU, is about 10 km to the east of the LE cluster, and the strong-motion station UU.MOR is essentially collocated with the LEs. Region U has slightly more earthquakes than the neighboring regions to the south (4 EQ vs. 22 EX), and the LEs are quite small. These factors lead to three FQ classifications and a relatively low specificity of 0.86. None of the four earthquakes were previously misclassified, giving a sensitivity of

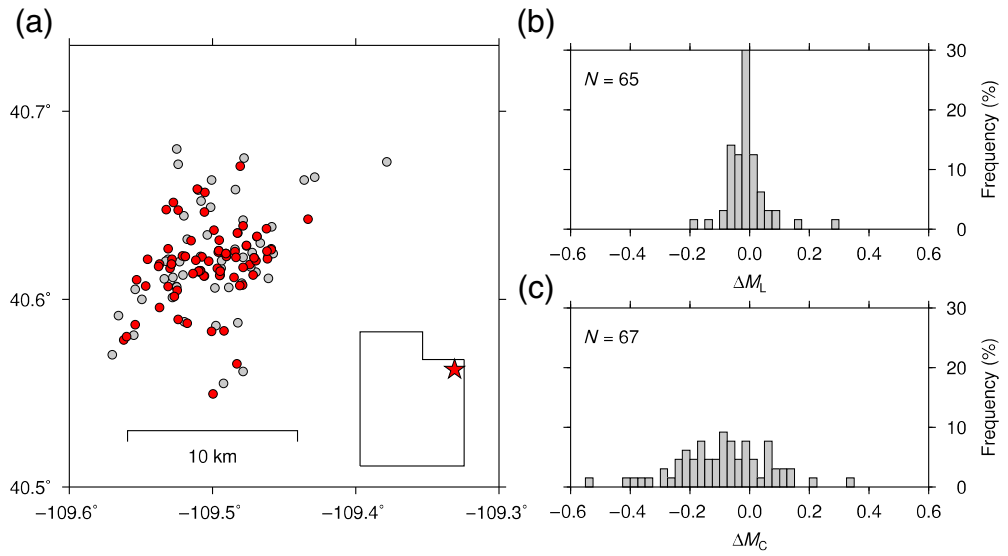

Figure 6. (a) Map of region R with explosions plotted to reflect their epicenters before (gray) and after (red) reanalysis. The location of region R within the Utah region is indicated by the red star on the inset image of the state. Changes in (b) M_L and (c) M_C during reanalysis. The color version of this figure is available only in the electronic edition.

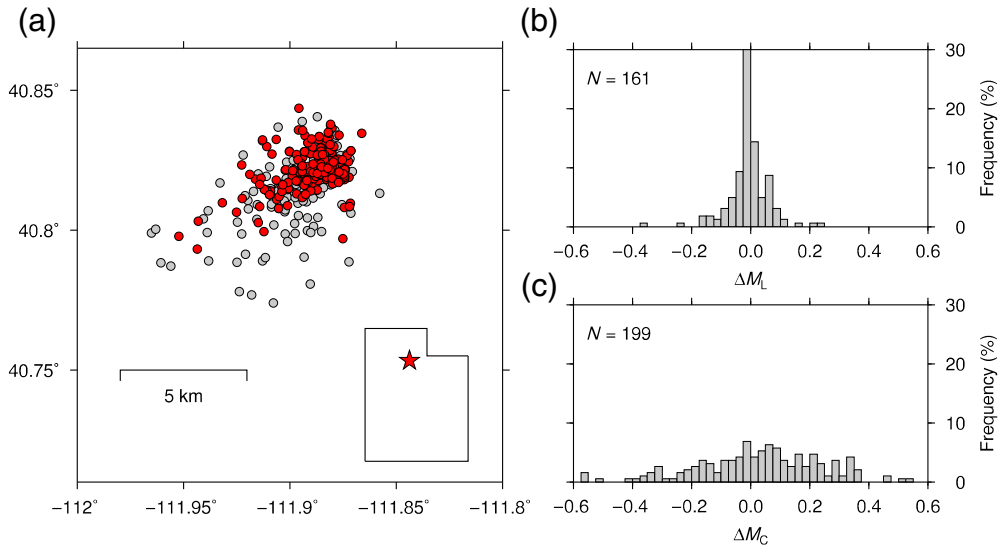

Figure 7. (a) Map of region T with explosions plotted to reflect their epicenters before (gray) and after (red) reanalysis. The location of region T within the Utah region is indicated by the red star on the inset image of the state. Changes in (b) M_L and (c) M_C during reanalysis. The color version of this figure is available only in the electronic edition.

1.00. Both M_L and M_C estimates were available for only 9 of the 22 LEs because of their small size.

Region V

Region V borders region U to the east and shares the same good station coverage. The waveforms from the eight earthquakes in this region are distinct from the waveforms of the 14 explosions, and none of the events were reclassified. Typical explosion waveforms with large-amplitude surface waves are best observed at broadband station UU.TCU, which is a few kilometers to the east. The earthquakes in the region have impulsive *S* waves at UU.TCU.

Region W

Region W is just west of the Great Salt Lake in northern Utah. It is on the western edge of the high-density portion of the UUSS seismic network, and the nearest broadband station, UU.SPU, is about 40 km to the northeast. Region W is home to the Hill Air Force Base's Utah Test and Training Range (UTTR). The UTTR is a Major Range and Test Facility run by the Department of Defense, which is remote enough to evaluate weapons that could be too impactful to test elsewhere (Hedlin *et al.*, 2012). In addition to the 178 analyzed explosions at UTTR, region W has a distinct cluster of events about 8 km north of the main UTTR blasting platform (Fig. 8). UTTR explosions from the main platform have waveforms with impulsive *P* waves, slightly less impulsive *S* waves at larger distances, and well-defined frequency changes between the two. The cluster to the north has emergent first arrivals.

The above-ground nature of these explosions means that surface waves (*Rg*) are not as effectively produced and discrimination is more difficult. We used stations UU.BGU, UU.SNUT, and UU.SPU for discrimination. UU.SPU records the least number of events but is the most useful in discrimination because the *S* wave is most prominent. Station coverage is poor in region W, with an AAG of 170. Most of the UTTR explosions occur at certain times of

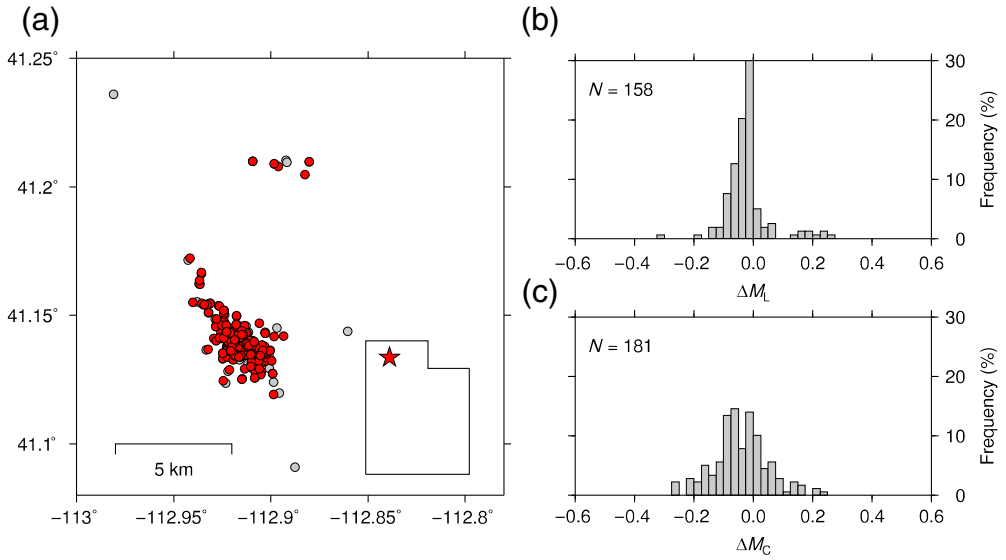

Figure 8. (a) Map of region W with explosions plotted to reflect their epicenters before (gray) and after (red) reanalysis. The location of region W within the Utah region is indicated by the red star on the inset image of the state. Changes in (b) M_L and (c) M_C during reanalysis. The color version of this figure is available only in the electronic edition.

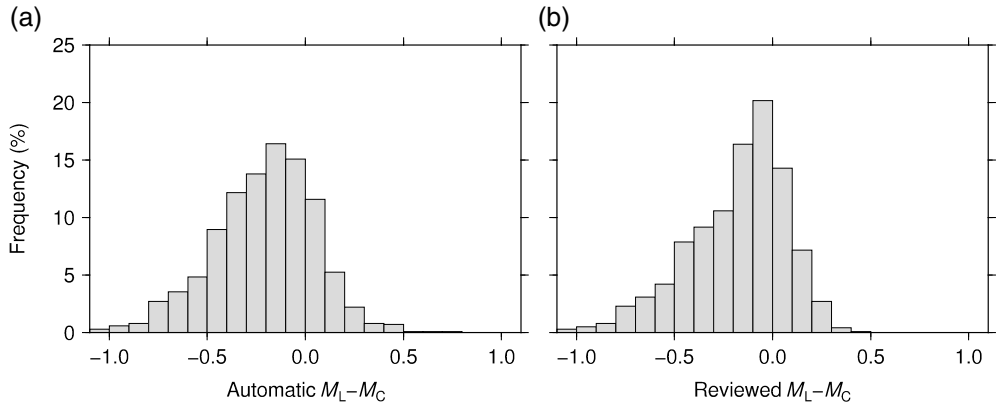

Figure 9. Histograms of M_L–M_C values for the same 1007 explosions in the Utah region (a) before reanalysis and (b) after reanalysis.

the day during certain months of the year. Though there are eight FQs in this region, the consistency in blasting origin time, high frequency of testing, and low rate of natural seismicity make discrimination straightforward. The availability of ground-truth information regarding UTTR explosions allowed us to fix the depths at −1.5 km.

Region X

Region X is located in a densely instrumented part of northern Utah. The nearest broadband station, UU.SPU, is about 20 km to the west. Three other stations, UU.GZU, UU.PCL, and UU.BES, are located with a few kilometers of the explosion cluster. Like region N, region X encompasses an earthquake swarm as well as the explosion cluster. The earthquake swarm was clearly recognized by analysts, so there are no reclassifications in this region. Seventy percent of the events in this region have an M_L and M_C measurement, which is likely a result of the relatively large size of the explosions.

Region Y

Region Y is about 20 km north of region X and is likewise densely instrumented. The closest station to the events in region Y (UU.BCU) is close to the average epicentral centroid; however, this station is usually too noisy to contribute to discrimination. Instead, we primarily relied on UU.WVUT, UU.LTU, and UU.HONU. The LEs in this area have dominant surface waves that make explosion sources obvious. The sensitivity was 1.00, and the specificity was 0.91.

Region Z

Region Z is located about 20 km west of region Y in northern Utah. The explosion cluster is about 40 km northeast of broadband station UU.SPU. Short-period station UU.LTU is essentially collocated with the LEs but event locations are hard to constrain because first arrivals are emergent and only propagate to a few nearby stations. The three FQ reclassifications (specificity of 0.77) are likely a consequence of clear *S* waves in the LE waveforms.

Discussion of M_L–M_C Observations for Utah Explosions

We present the original and revised M_L–M_C distributions for the same group of 1007 reanalyzed explosions in Figure 9. The revised distribution is more asymmetrical and less biased than the original distribution. The shift in M_L–M_C that occurred

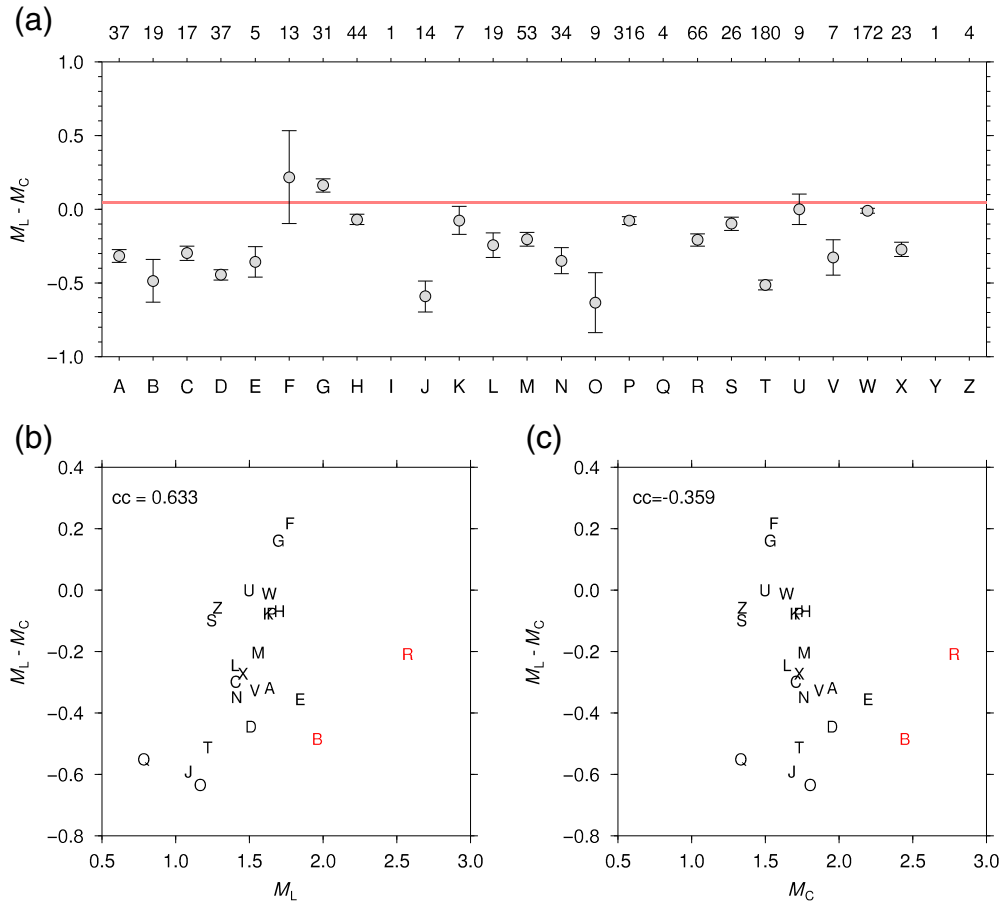

Figure 10. (a) Average M_L–M_C values for analyst reviewed explosions in the Utah region. The letters across the bottom correspond to boxed regions in Figure 1, and the numbers across the top indicate the number of explosions in each region. The error bars represent 95% confidence intervals. The red line is the 95% confidence interval for naturally occurring earthquakes in the Utah region. Average M_L–M_C plotted against average (b) M_L and (c) M_C for the 22 regions with $N > 4$ observations. In both cases, regions R and B (red font) were omitted from the correlation coefficient (cc) calculation. The color version of this figure is available only in the electronic edition.

during reanalysis reflects larger revisions to M_C than to M_L (Figs. 4–8), likely because peak-to-peak amplitude picks are simpler to make than choosing coda duration windows. The changes in M_C values are mostly due to the redetermination of the signal duration, as the human-reviewed duration is often very different than the automatic-solution since the automatic-solution was calibrated for earthquakes, not explosions. M_C values are also changed through relocation, as relocation changes the epicentral distance, but these changes are minimal relative to the change in M_C from reevaluated signal duration measurements. During reanalysis the number of explosions with both M_L and M_C grew to 1148, with a mean of -0.196 ± 0.017 (95% confidence interval). Previous work in Utah found a mean M_L–M_C value of -0.137 ± 0.008 for likely explosions and a mean value of 0.048 ± 0.008 for naturally occurring tectonic earthquakes, which dominantly occur at depths of 5–15 km (Koper *et al.*, 2016). Hence, the work presented here corroborates the usefulness of M_L–M_C as a crustal depth discriminant in Utah, helping to distinguish extremely shallow seismic events from deeper, naturally occurring earthquakes.

It is interesting to consider how M_L–M_C varies regionally since there is a range of source types, propagation paths, and site effects across the Utah region. In Figure 10, we present M_L–M_C mean values and 95% confidence intervals for each region with at least five M_L–M_C observations. Of the 22 regions that meet this requirement, 19 have M_L–M_C means that are more negative than the overall earthquake mean at confidence levels above 95%. Two regions (F and U) have M_L–M_C 95% confidence intervals that include the earthquake range. Only region G has an M_L–M_C 95% confidence interval that is more positive than the earthquake range.

M_L–M_C has a stronger dependence on M_L than M_C (Fig. 10). Events with larger M_L tend to have larger, more earthquake-like values of M_L–M_C. We attribute this to UUSS network processing techniques. All of the individual station M_C values are averaged to calculate the event M_C. Any station M_C value is discarded from the calculation of the event M_C if it differs by more than 0.8 magnitude units from the event M_C. This leads to a distance dependence of M_C. Small events are only recorded by nearby stations, and those seismograms tend to have anomalously long durations relative to typical peak-to-peak amplitudes because *Rg* energy, which is strong at close distances, extends duration more than it increases amplitude (M_C is increased relative to M_L). Large events are mostly recorded at farther stations where *Rg* is less observable, so waveforms tend to have more typical durations and M_C and M_L are in agreement. In other words, the distance dependence of the UUSS M_C formula is too weak to account for the true distance-dependent change in coda energy from explosions. If these anomalously large station M_C values were not eliminated from the event averages, many regions

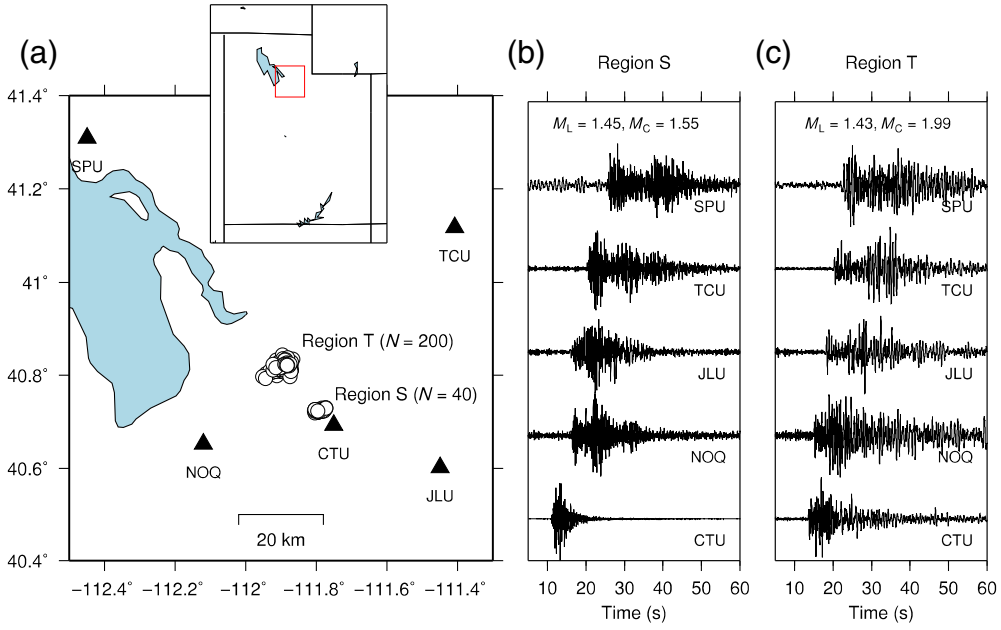

Figure 11. (a) Comparison of typical explosion waveforms from two nearby quarries in north central Utah. The location of this region within Utah is indicated by the red box on the inset image of the state. The (b) region S explosion occurred on 3 November 2012 13:49:23 (UTC) and (c) region T explosion occurred on 27 November 2012 14:55:04 (UTC). Events from region T generally have anomalously large M_C values, while those from region S have more earthquake-like M_L–M_C values. All traces are proportional to vertical-component ground velocity in a 1–10 Hz passband. The color version of this figure is available only in the electronic edition.

(such as P) would have more negative M_L–M_C values. The relatively high values of M_L–M_C in regions F, U, and G noted earlier corroborate this network processing explanation. Other source-specific factors also play a role in the regional variation of M_L–M_C. For instance, regions K and W have 95% confidence intervals for M_L–M_C that are only slightly below the earthquake range. These are the two regions that contain above-ground explosions. The weak coupling to the solid Earth leads to less efficient *Rg* excitation, which in turn leads to shorter codas and more positive M_L–M_C values.

The clearest example of source-related M_L–M_C variation comes from a comparison between regions S and T (Fig. 11). These two regions are separated by only about 15 km and produce similarly sized quarry blasts with 26 events in region S having a mean M_L of 1.24 ± 0.052, and 180 events in region T having a mean M_L of 1.21 ± 0.036. Yet, region S has a mean M_L–M_C of −0.098 ± 0.046, while region T has a mean M_L–M_C of −0.512 ± 0.333. Waveform differences from the two regions occur over a range of distances and azimuths (Fig. 11), implying that the difference is not caused by geologic variations along source-to-receiver paths but rather by variations in the source region.

There are two likely source-related explanations for the waveform variations observed in regions S and T. The first explanation is that the mine in region T may use more shot holes on average than the mine in region S. Increasing the number of shot holes increases the source-time function without affecting the maximum amplitude of the explosion. As the duration of the source-time function approaches the dominant period of *Rg* (0.5–2 s), *Rg* is increasingly excited leading to longer duration waveforms (Kim *et al.*, 1994). The second explanation involves near-source geology. Region T is geologically heterogeneous, with deformed Mississippian limestones overlain by extensive conglomerates. It lies within the mature Wasatch fault damage zone, along the boundary between the Salt Lake City sedimentary basin to the southwest and the Wasatch Mountains to the northeast. Such near-source sediment is thought to enhance *P*-to-*S* conversion (Kim *et al.*, 1994), leading to longer coda duration. Region S, in contrast, is on the axis of the ductilely deformed Parley's Canyon Syncline, a structure composed of competent, laterally homogeneous Jurassic limestones, more distant from the basin. Determining the relative balance of these two effects requires obtaining detailed blasting patterns from the mines and performing high-frequency waveform simulation in realistic Earth models, which we leave for future work.

Conclusions

We manually refined the locations and magnitudes of 1545 explosions that occurred in the Utah region between 1 October 2012 and 30 June 2018. M_L values vary from 0.65 to 2.90 with a median of 1.58, and M_C values vary from 0.35 to 3.15 with a median of 1.68. Most of the explosions are delay-fired, near-surface mine blasts, although some single-fired, above-ground blasts related to military activities are also included. The new catalog is intended to be used by researchers in verification seismology working on methods of low-yield nuclear monitoring. While methods of classifying moderate-sized (**M** 3–5) seismic events recorded at regional distances (~200–2000 km) are well established (National Research Council, 2012), it is unclear whether the same methods are effective for small seismic events (**M** 0–2) recorded at local distances (<200 km) or whether new discriminants need to be developed.

We used the new catalog to confirm the effectiveness of M_L–M_C as a depth discriminant in the Utah region. A total of 1148 explosions in the new catalog were well recorded enough to have both M_C and M_L calculated. The mean M_L–M_C value for the explosions is -0.196 ± 0.017 (95% confidence interval), significantly more negative than the M_L–M_C value of 0.048 ± 0.008 previously observed for naturally occurring earthquakes in Utah (Koper *et al.*, 2016). We attribute the negative M_L–M_C values of explosions to their shallow depth, which preferentially excites local surface waves (*Rg*) that scatter and disperse within the low-velocity, strongly heterogeneous, shallow crust, thus generating abnormally long-duration coda waves.

We observed significant variation in M_L–M_C among 26 distinct explosion source regions in and around Utah. The most negative value of -0.634 ± 0.204 was observed for nine explosions from a quarry in north-central Utah, and the most positive value of 0.218 ± 0.314 was observed for 13 explosions from a quarry in southwestern Utah. However, even nearby source regions could have significantly different values because of different blasting practices or geologic setting. Two explosion source regions near Salt Lake City that are separated by just 15 km had mean M_L–M_C values that differed by 0.414 ± 0.336. To achieve the best discrimination results, M_L–M_C observations should be combined with other, preferably noncorrelated, local discriminants in a mathematically rigorous manner, perhaps similar to the methodology used to combine regional-to-teleseismic discriminants (Anderson *et al.*, 2007).

Data and Resources

The seismic data used in this study are publicly available from the Incorporated Research Institutions for Seismology (IRIS) Data Management Center at www.iris.edu. The program HYPOINVERSE is available from the U.S. Geological Survey (USGS) at https://earthquake.usgs.gov/research/software. The catalog of explosion source parameters is available by email request to Keith D. Koper (koper@seis.utah.edu). Many of the figures were made using Generic Mapping Tools (GMTs; Wessel and Smith, 1998). The online reports of University of Utah Seismograph Stations (UUSS) can be accessed at quake.utah.edu. Dugway Proving Ground can be accessed at www.dugway.army.mil. The Utah Division of Oil, Gas, and Mining website can be accessed at www.ogm.utah.gov. All websites were last accessed in June 2019.

Acknowledgments

This study was funded by the Air Force Research Laboratory under Contract FA9453-17-C-0022. The authors thank Jim Pechmann, Kim McCarter, and two anonymous reviewers for comments and suggestions.

References

Allmann, B. P., P. M. Shearer, and E. Hauksson (2008). Spectral discrimination between quarry blasts and earthquakes in southern California, *Bull. Seismol. Soc. Am.* **98,** 2073–2079, doi: 10.1785/0120070215.

Anderson, D. N., D. K. Fagan, M. A. Tinker, G. D. Kraft, and K. D. Hutchenson (2007). A mathematical statistics formulation of the teleseismic explosion identification problem with multiple discriminants, *Bull. Seismol. Soc. Am.* **97,** 1730–1741, doi: 10.1785/0120060052.

Arrowsmith, S. J., M. D. Arrowsmith, M. A. H. Hedlin, and B. Stump (2006). Discrimination of delay-fired mine blasts in Wyoming using an automatic time-frequency discriminant, *Bull. Seismol. Soc. Am.* **96,** 2368–2382.

Astiz, L., J. A. Eakins, V. G. Martynov, T. A. Cox, J. Tytell, J. C. Reyes, R. L. Newman, G. H. Karasu, T. Mulder, M. White, *et al.* (2014). The array network facility seismic bulletin: products and an unbiased view of United States seismicity, *Seismol. Res. Lett.* **85,** 576–593, doi: 10.1785/0220130141.

Baumgardt, D. R., and K. A. Ziegler (1988). Spectral evidence for source multiplicity in explosions: application to regional discrimination of earthquakes and explosions, *Bull. Seismol. Soc. Am.* **78,** 1773–1795.

Block, L. V., C. K. Wood, W. L. Yeck, and V. M. King (2015). Induced seismicity constraints on subsurface geological structure, Paradox Valley, Colorado, *Geophys. J. Int.* **200,** 1172–1195.

Bowers, D., and N. D. Selby (2009). Forensic seismology and the comprehensive Nuclear-Test-Ban Treaty, *Annu. Rev. Earth Planet. Sci.* **37,** 209–236.

Gibbons, S. J., and F. Ringdal (2006). The detection of low magnitude seismic events using array-based waveform correlation, *Geophys. J. Int.* **165,** 149–166.

Goforth, T. T., and J. L. Bonner (1995). Characteristics of R_g waves recorded from quarry blasts in Central Texas, *Bull. Seismol. Soc. Am.* **85,** 1232–1235.

Hedlin, M. A. H., C. de Groot-Hedlin, and D. Drob (2012). A study of infrasound propagation using dense seismic network recordings of surface explosions, *Bull. Seismol. Soc. Am.* **102,** 1927–1937.

Holt, M. M., K. D. Koper, W. Yeck, S. d'Amico, Z. Li, J. M. Hale, and R. Burlacu (2019). On the portability of M_L-M_C as a depth discriminant for small seismic events recorded at local distances, *Bull. Seismol. Soc. Am.* **109,** no. 5, 1661–1673.

Kim, W.-Y., D. W. Simpson, and P. G. Richards (1994). Discrimination of earthquakes and explosions in the eastern United States using regional high-frequency data, *Geophys. Res. Lett.* **20,** 1507–1510.

King, V. M., L.V. Block, and C. K. Wood (2016). Pressure/flow modeling and induced seismicity resulting from two decades of high-pressure deep-well brine injection, Paradox Valley, Colorado, *Geophysics* **81,** 119–134.

Klein, F. W. (2002). User's guide to HYPOINVERSE-2000, a Fortran program to solve for earthquake locations and magnitudes, *U.S. Geol. Surv. Open-File Rept. 2002–171*, 123 pp.

Koper, K. D., J. C. Pechmann, R. Burlacu, K. L. Pankow, J. Stein, J. M. Hale, P. Roberson, and M. K. McCarter (2016). Magnitude-based discrimination of man-made seismic events from naturally occurring earthquakes in Utah, USA, *Geophys. Res. Lett.* **43,** 10,638–10,645.

Linville, L., K. Pankow, and T. Draelos (2019). Deep learning models augment analyst decisions for event discrimination, *Geophys. Res. Lett.* **46,** 3643–3651.

National Research Council (1998). *Seismic Signals from Mining Operations and the Comprehensive Test Ban Treaty: Comments*

on a Draft Report by a Department of Energy Working Group, The National Academies Press, Washington, D.C., doi: 10.17226/6226.

National Research Council (2012). *The Comprehensive Nuclear Test Ban Treaty: Technical Issues for the United States*, The National Academies Press, Washington, DC, doi: 10.17226/12849.

Pankow, K. L., S. Potter, H. Zhang, and J. Moore (2017). Local seismic monitoring at the Milford, Utah FORGE site, *Geotherm. Res. Council Trans.* **41,** 304–312.

Pechmann, J. C., S. J. Nava, F. M. Terra, and J. C. Bernier (2007). Local magnitude determinations for Intermountain Seismic Belt earthquakes from broadband digital data, *Bull. Seismol. Soc. Am.* **97,** 557–574.

Richards, P. G., D. A. Anderson, and D. W. Simpson (1992). A survey of blasting activity in the United States, *Bull. Seismol. Soc. Am.* **82,** 1416–1433.

Stump, B., R. Burlacu, C. Hayward, J. Bonner, K. Pankow, A. Fisher, and S. Nava (2007). Seismic and infrasound energy generation and propagation at local and regional distances: Phase I-Divine Strake experiment, in *Proc. of the 29th Monitoring Research Review: Ground-Based Nuclear Explosion Monitoring Technologies*, U.S. Dept. of Energy, Denver, LA-UR-07-5613, Vol. 1, 674–683.

Stump, B. W., M. A. H. Hedlin, D. C. Pearson, and V. Hsu (2002). Characterization of mining explosions at regional distances: Implications with the international monitoring system, *Rev. Geophys.* **40,** 2-1–2-21, doi: 10.1029/1998RG000048.

Tibi, R., K. D. Koper, K. L. Pankow, and C. J. Young (2018). Depth discrimination using R_g-to-S_g spectral amplitude ratios for seismic events in Utah recorded at local distances, *Bull. Seismol. Soc. Am.* **108,** 1355–1368.

University of Utah (1962). University of Utah Regional Seismic Network, *International Federation of Digital Seismograph Networks, Other/Seismic Network*, doi: 10.7914/SN/UU.

Wessel, P., and W. H. F. Smith (1998). New, improved version of generic mapping tools released, *Eos Trans. AGU* **79,** 579, doi: 10.1029/98EO00426.

Wiemer, S., and M. Baer (2000). Mapping and removing quarry blast events from seismicity catalogs, *Bull. Seismol. Soc. Am.* **90,** 525–530.

Yeck, W. L., L. V. Block, C. K. Wood, and V. M. King (2015). Maximum magnitude estimations of induced earthquakes at Paradox Valley, Colorado, from cumulative injection volume and geometry of seismicity clusters, *Geophys. J. Int.* **200,** 322–336.

Zeiler, C., and A. A. Velasco (2009). Developing local to near-regional explosion and earthquake discriminants, *Bull. Seismol. Soc. Am.* **99,** 24–35.

Manuscript received 18 July 2019
Published online 6 November 2019